

Scanning magnetoresistive microscopy for die-level sub-micron current density mapping

B. D. Schrag, X. Y. Liu, M. J. Carter, and Gang Xiao
Micro Magnetics Inc., Providence, RI

Abstract

In this paper, we will present a new technique for fault isolation and failure analysis in integrated circuits based on a scanning magnetoresistive imaging system. By detecting the stray magnetic fields at the surface of a chip using magnetic sensors with sub-micron spatial resolution, we are able to obtain a full map of in-plane current densities, resolving features smaller than 100 nanometers. We will briefly discuss the capabilities and limitations of the technique and will present results on a variety of frontside and backside samples.

Introduction

Magnetic imaging techniques have found numerous practical applications in many areas of science and technology [1]. In addition, recent advances in the emerging field of spintronics have created new and powerful magnetic devices with the potential to have a significant impact on both industry and academia. Sensors based on the giant magnetoresistance (GMR) effect, first discovered in 1987, have already become the standard in the personal computer hard-disk drive (HDD) market, while an even newer type of sensor, the magnetic tunnel junction (MTJ), discovered in the mid-1990s, has been shown to have several significant advantages over GMR technology. We have built on these sensing technologies to develop a new imaging tool for mapping current densities in thin film conductors. Our tool is non-invasive, operates under ambient conditions, and is capable of spatial resolution better than 100 nm. In this paper, we will discuss the application of this tool for the purposes of fault isolation and failure analysis in integrated circuits.

Experimental Details

The basic operation of our system has been described elsewhere [2] and will be briefly summarized here. A magnetic sensing element is raster scanned either in contact with or at a fixed height above the sample. The sample can be driven using a wide variety of powering options. The sensor output is boosted using one of several preamplification circuits built into the on-board electronics, and the amplified signal is

demodulated and sampled in real-time by a data acquisition board. Data is acquired in either a time-based or encoder-based manner, depending on the particulars of the scan. After the magnetic field map is acquired, we use a modified form of an algorithm developed by Roth [3] to create a map of current densities.

We use magnetoresistance-based sensors to measure the vertical component of magnetic field at the surface. Sensor packages based on both magnetoresistive (MR) and magnetic tunnel junction (MTJ) sensors are manufactured in-house. The choice of sensor is dependent on the application. Our sensors are designed for both front side and flip chip applications. More information about our sensor design and performance can be found elsewhere [4-5].

Results

Mouse bites in a quarter-micron-pitch conductor

We will illustrate the technique with a number of examples, starting with simple test structures and continuing on to scans of operational IC samples. Figure 1 displays results taken on a quarter-micron-pitch test structure. The scan was made in contact mode, with an estimated distance between the current-carrying layer and the sensor of 200 nm. Figure 1(a) shows the raw magnetic field image above this sample, with large positive (negative) magnetic fields represented by areas of red (blue). Figure 1(b) maps the current density $J (= \sqrt{J_x^2 + J_y^2})$ of the same area plotted using the same color scheme. This sample was fabricated with a physical defect in one edge with a width of one-half of the conductor pitch (125 nm). The resulting anomaly in current flow is easily seen in Fig 1(b), and a zoomed-in view of this area is shown in Fig 1(c). We also imaged an identical sample with a similar, yet smaller (63 nm) defect. The presence of the smaller defect was readily apparent from the field data, although its signature in the current density maps was less striking than that of the defect seen in Fig 1(b).

In order to detect very small perturbations in current density, such as those created by "mouse bites", both the sensor resolution (set by its active area) and the sensor-to-sample distance z are critical; as a rule of thumb, the *larger* of these two values limits the resolution of the technique. In this case,

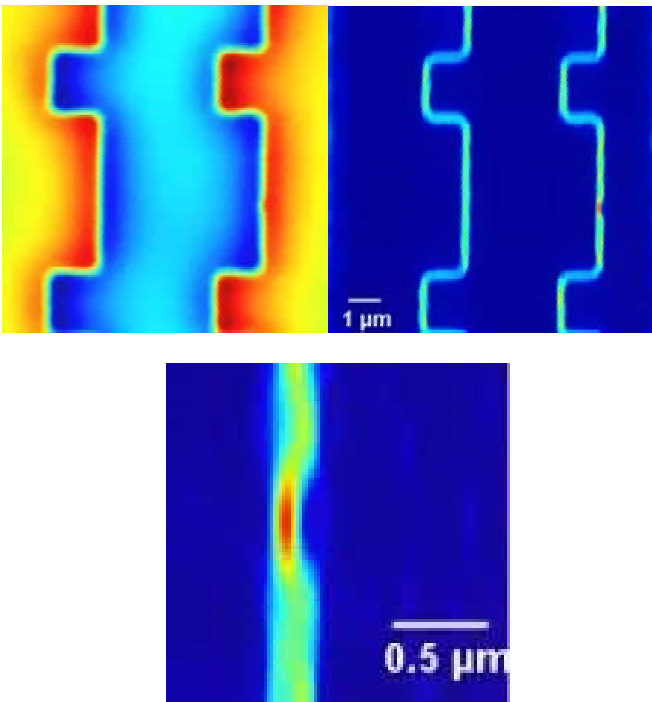


Figure 1: (a) False-color representation of the magnetic stray field above a quarter-micron-pitch patterned conductor. (b) Calculated current density map of the same $10 \times 10 \mu\text{m}$ area. (c) Zoomed-in view of the current density near a 125 nm mouse bite defect.

the intrinsic resolution in the primary scan direction is less important than z , which is nearly as large as the defect size. In this case, we have found that for defects of size d , detection is straightforward if the ratio z/d is smaller than ~ 3 , while a sufficient signal-to-noise ratio (SNR) and careful examination allows detection of much smaller defects down to $z/d \sim 6-10$.

Localization of breakdown in a cross-point array

Figure 2(a) shows the CAD layout of a test structure for investigating dielectric breakdown. This sample consists of two perpendicular arrays of metal fingers (width $1 \mu\text{m}$, spacing $1 \mu\text{m}$) separated by a thin layer of insulating material. This cross-point architecture creates a two-dimensional array of pixels at which the two metal layers overlap; this array is seen in the lower right of the CAD image. Under normal conditions, this structure is non-conductive, but the sample which was scanned showed a resistance of $\sim 400 \Omega$, indicating a probable breakdown of the dielectric layer. Figure 2(b) shows the raw magnetic field map at the surface of this sample as scanned using an MR sensing element. In this case, the field map immediately shows the nature of the failure, as the magnetic field signature pinpoints a single defective pixel as in (c). The sample was powered at $300 \mu\text{A RMS}$ at 500 kHz for this scan.

Current mapping in an operational logic chip

We have also imaged current densities in operating integrated circuits. Figure 3(a) shows an optical image of section of a

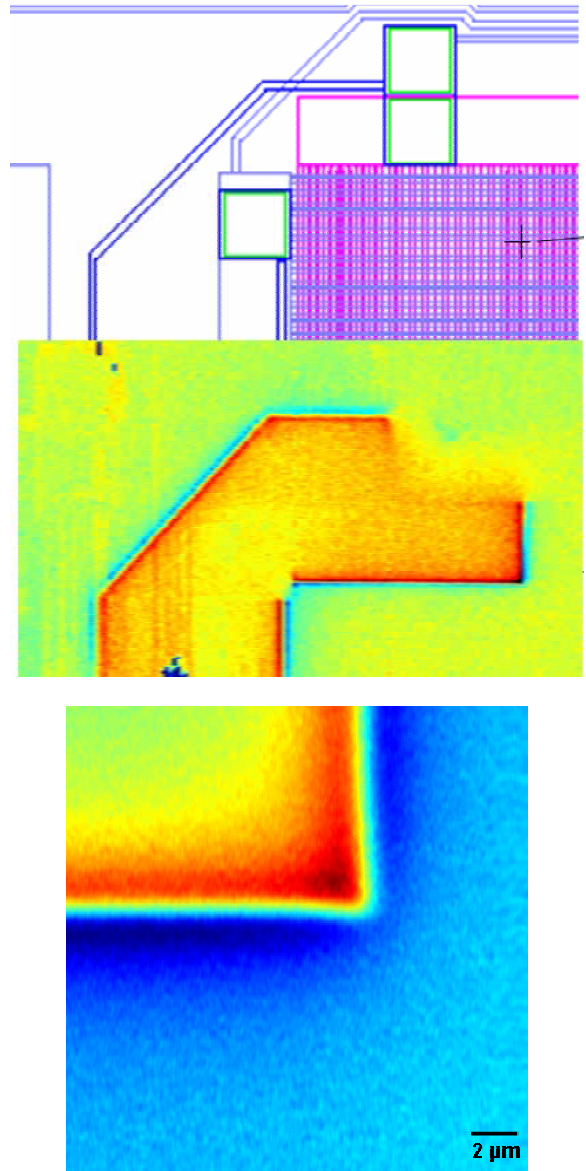


Figure 2: (a) Above: CAD image of a cross-point test structure. (b) Middle: Raw magnetic field image above the sample provides the "smoking gun" by localizing the failed pixel. (c) A zoom-in on the failed area localizes the exact location of current transition between levels to within one micron.

logic chip. Figure 3(b) shows the current density map of this same area which was reconstructed from the stray magnetic field data. This scan, taken with a magnetoresistive sensing element in contact with the sample, covered an area of 9 mm^2 with micron-scale resolution.

IC samples can be imaged in a number of other ways; for example, by powering the chip normally while applying the AC modulation to a pin other than the power pin, which will allow visualization of the current flow only in a selected section of the sample. We have used this method to image current through sets of pins whose electrical characteristics are

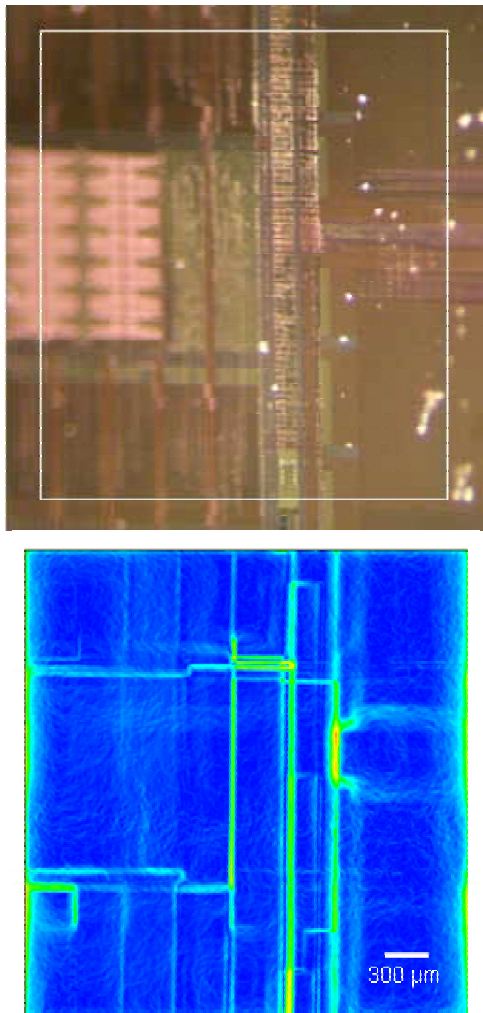


Figure 3: (a) Above: optical image of a small section (~3x3 mm) of an operational logic chip and (b) Below: current density map of the same area.

found to deviate from expected values. In many cases, the current distribution in a given sample may be very complicated; therefore, the best way to diagnose a fault is often to compare the current distribution of the failed device to that of a known good chip. Many chips have on-board components which filter out high-frequency signals, so care must be taken to choose a frequency which is low enough to be admitted into the inner workings of the IC. Alternatively, the sample can be powered in a way which circumvents such elements. Our sensors have an extremely wide operating frequency range, from DC up to several GHz, which usually allows the selection of an appropriate frequency.

Figure 4 shows the optical and current density images taken on an operating SRAM sample powered at 2.5VDC with a AC 200 mVRMS voltage. The current enters the sample at two wire bond pads, seen to the left of the optical image. To obtain good results, it is often easiest to begin imaging by scanning the area where current first enters the multilayer structure, such as at a bond pad, and then to follow the current throughout the chip, until it disperses or disappears into the

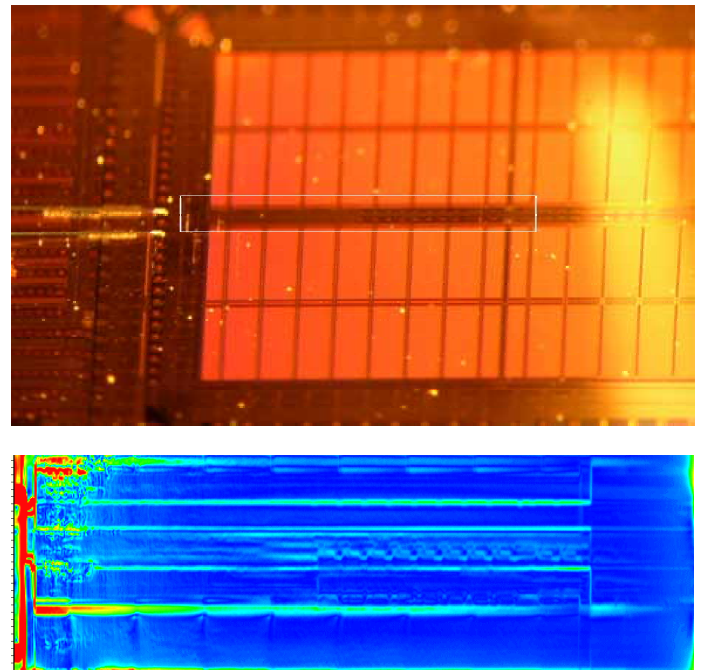


Figure 4: (a) Zoomed-in optical image of an operating SRAM sample. The white box indicates the region of interest (with the true aspect ratio). (b) Current density image of this ROI. This map is presented with a skewed aspect ratio for clarity.

lower levels of the package. In the sample shown in Figure 4, the current amplitude can be seen to slowly wane as it flows toward the right edge of the image. This indicates that the current is leaking off through many of the active components into the die, as opposed to shorting all at once through a single location.

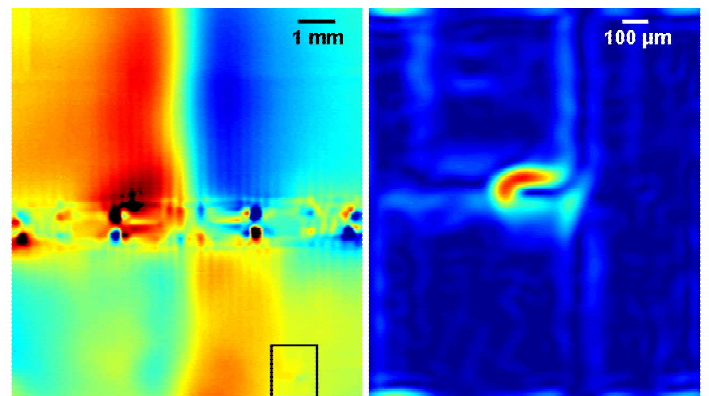


Figure 5: Left: Magnetic field distribution of the full die of a flip-chip sample. The strong field signatures across the center of the package are created by the introduction of power from the package level to the chip itself. Right: Current density image of a FIB-induced short at the lower right of the sample (the location of this area is indicated by the black box in the first image).

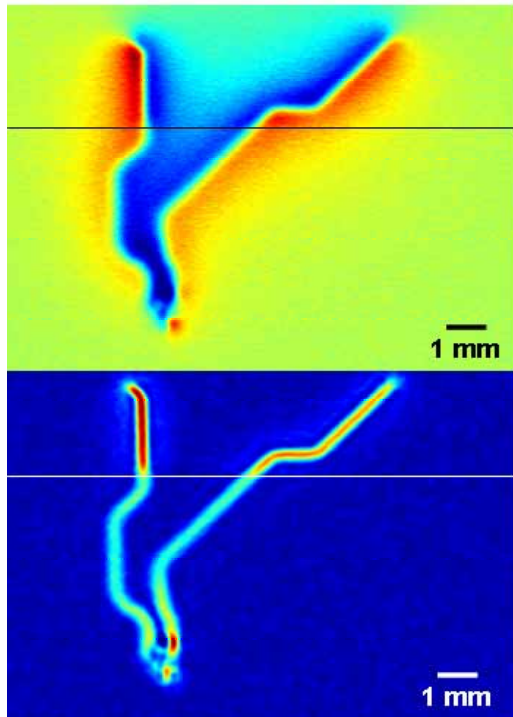


Figure 6: Field image and current density map of a flip-chip test structure. The current enters at a point in the package near the top left of the image and then flows into a test structure on the die, before exiting through another point at the top right. The horizontal lines on each image indicate the boundary of the die.

Imaging of flip-chip samples and packages

We have also imaged samples in a flip-chip configuration. The relatively large separation between the current-carrying layers and the magnetic sensor ($\sim 100 \mu\text{m}$) limits the spatial resolution of the technique in comparison with front side scanning. However, for many types of failures, this reduced resolution is sufficient to make a clear diagnosis of the problem. Figures 5 and 6 show results obtained on two such samples. These images were acquired using an MR sensor fabricated in-house with a voltage sensitivity over twenty times better than our magnetoresistive sensors. This increase in sensitivity allows for much faster scan rates and for the detection of smaller current densities. Figure 5 gives the magnetic field profile of an SRAM chip with a FIB-induced short. The short appears as a faint field signature in the lower right of the die in Figure 5(a), but is readily imaged with a more detailed scan, as in Fig. 5(b). This sample carries a $900 \mu\text{A}$ RMS AC current. Figure 6, in comparison, displays the current density profile of an entire flip-chip device and the adjacent package area. This sample carries a $700 \mu\text{A}$ RMS AC current. In Figure 6, the location of the current path can be clearly traced through the entire chip, and can therefore be compared with the chip layout to localize potential problems.

Conclusions and Future Work

We have demonstrated promising applications of a new current-mapping technology based on miniaturized spintronics-based magnetic sensors. The high spatial resolution of our sensors allows us to resolve features down to 50 nm . For front-side applications, we can expect deep submicron resolution in most cases, and the technique has the advantages of operation at ambient conditions and non-invasiveness.

Acknowledgements

The authors wish to thank Wayne Ford, Mike McIntyre, Dave Vallett, and Zhiyong Wang for samples and technical assistance. We also wish to thank Dave Vallett and Zhiyong Wang for helpful discussions.

References

1. M. R. Freeman and B. C. Choi, *Advances in magnetic microscopy*, *Science*, 294, 1484 (2001).
2. B. D. Schrag and Gang Xiao, *Submicron electrical current density imaging of embedded microstructures*, *Appl. Phys. Lett.*, 82, 3272 (2003).
3. B. J. Roth, N. G. Sepulveda, and J. P. Wikswo, Jr., *Using a magnetometer to image a two-dimensional current distribution*, *J. Appl. Phys.* 65, 361 (1989).
4. X. Y. Liu, C. Ren, and Gang Xiao, *Magnetic tunnel junction sensors with a hard-axis bias field*, *J. Appl. Phys.* 92, 4722 (2002).
5. X. Y. Liu and Gang Xiao, *Thermal annealing effects on low-frequency noise and transfer behavior in magnetic tunnel junction sensors*, submitted to *Appl. Phys. Lett.* (2003).